Cell Research (2014) 24:1288-1298.

www.nature.com/cr

ORIGINAL ARTICLE

Induction of entosis by epithelial cadherin expression

Qiang Sun[1, 2], Edmund S Cibas[3], Hongyan Huang[4], Louis Hodgson[5], Michael Overholtzer[2, 6]

[1]Laboratory of Cell Engineering, Institute of Biotechnology, Beijing 100071, China; [2]Cell Biology Program, Memorial Sloan-Kettering Cancer Center, New York, NY 10065, USA; [3]Department of Pathology, Brigham and Women's Hospital and Harvard Medical School, Boston, MA 02115, USA; [4]Department of Oncology, Beijing Shijitan Hospital of Capital Medical University, 10 TIEYI Road, Beijing 100038, China; [5]Department of Anatomy and Structural Biology and Gruss-Lipper Biophotonics Center, Albert Einstein College of Medicine of Yeshiva University, Bronx, NY, USA; [6]BCMB Allied Program, Weill Cornell Medical College, 1300 York Avenue, New York, NY 10065, USA

Cell engulfment typically targets dead or dying cells for clearance from metazoan tissues. However, recent evidence demonstrates that live cells can also be targeted and that engulfment can cause cell death. Entosis is one mechanism proposed to mediate the engulfment and killing of live tumor cells by their neighbors, an activity often referred to as cell cannibalism. Here we report that the expression of exogenous epithelial cadherin proteins (E- or P-cadherin) in human breast tumor cells lacking endogenous expression of epithelial cadherins induces entosis and inhibits transformed growth. Entosis induced by cadherin expression is associated with the polarized distribution of Rho and Rho-kinase (ROCK) activity within entotic cells, which is dependent on p190A RhoGAP activity. ROCK inhibition or downregulation of p190A RhoGAP expression reduces entosis and increases the transformed growth of epithelial cadherin-expressing tumor cells. These data define new cell systems for the study of entosis, and identify entosis as a mechanism of cell cannibalism that is induced by the establishment of epithelial adhesion and inhibits transformed growth.

***Keywords*:** entosis; cadherin; Rho GTPase; actomyosin; p190A RhoGAP; tumor suppression

Cell Research (2014) **24**:1288-1298. doi:10.1038/cr.2014.137; published online 24 October 2014

Introduction

The role of cell engulfment in metazoan programmed cell death is traditionally viewed as downstream of the autonomous commitment of cells to die. In this model, professional or nonprofessional phagocytes respond to "find-me" and "eat-me" signals emitted by dying cells to clear the dead cells, and thereby protect tissues from the potential adverse effects of unengulfed cells, such as inflammation linked to cell leakage (or called secondary necrosis) [1]. While cell engulfment clearly functions downstream of cell death in many contexts, recent evidence also places cell engulfment upstream of cell death in some circumstances, suggesting that cell engulfment may not simply function to clean up dying cells but could also regulate rates of cell death. Phagocytes play a facilitating role in developmentally programmed apoptotic death in *C. elegans* [2, 3], and phagocytic glial cells and macrophages have been shown to clear otherwise viable cells that are targeted due to the exposure of "eat-me" signals or the loss of "don't-eat-me" signals such as CD47 [4, 5].

Engulfment of viable cells by human tumor cells, commonly called cell cannibalism or cell-in-cell formation, has been observed for many years [6]. Cell cannibalism has been shown to occur most frequently in high-grade or metastatic tumors [7-9], suggesting that it may promote tumor progression. It has been shown that cannibalism can support tumor cell survival or proliferation under starvation stress [8, 10], promote ploidy changes [7, 11], and affect clonal selection by mediating competition between tumor cells (see the companion paper by Sun *et al*. [12]). Alternatively, cell cannibalism could

Correspondence: Michael Overholtzer[a], Qiang Sun[b]
[a]Tel: +1 212-639-6536; Fax: +1 212-794-4342
E-mail: overhom1@mskcc.org
[b]Tel: 86-10-66948820
E-mail: sunqiang1975@126.com
Received 31 December 2013; revised 7 March 2014; accepted 30 July 2014; published online 24 October 2014

be tumor-suppressive in some contexts as the ingestion of tumor cells by their neighbors induces tumor cell death, leading to limited transformed growth [13, 14]. While the effects of cell cannibalism on tumor cells are becoming known, the mechanism by which tumor cells cannibalize remains unclear, with no consensus working model except that cannibalism is frequently argued to be nonphagocytic in nature [6, 15, 16].

One mechanism proposed to underlie homotypic cannibalism, where tumor cells ingest neighboring tumor cells, is called entosis. By entosis, tumor cells utilize the machinery of cell-cell adhesion and the actomyosin cytoskeleton to drive engulfment [13]. Engulfment by this mechanism requires epithelial E- or P-cadherins and Rho-GTPase signaling specifically within ingested cells, suggesting that cell engulfment after the formation of cell adhesions is due to the increased actomyosin contraction in ingested cells that promotes their uptake [13]. Cannibalistic cell structures observed in primary human breast tumor cells exhibit β-catenin localization patterns that are indicative of a cell junction-mediated mechanism of engulfment, suggesting that entosis occurs *in vivo* [13]. However, other mechanisms not involving Rho signaling or E-cadherin are also proposed to mediate tumor cell cannibalism, including a recently described phagocytosis-like process occurring between pancreatic tumor cells, which involves Cdc42 [15, 17, 18].

To further explore the mechanism underlying cell cannibalism, we investigated human breast tumor cells and found that spontaneous cell cannibalism is rare in most tumor cell lines owing in part to a lack of epithelial cadherin expression. We therefore attempted to use a "gain-of-function" approach to establish a cell model with increased cadherin expression in order to further study entosis. Indeed, breast tumor cells engineered to express exogenous E- or P-cadherins establish epithelial junctions, and engulf and kill their siblings, leading to suppression of transformed growth. The inhibition of Rho-kinases (ROCKs) reduces engulfment and restores transformed growth, supporting a model whereby entosis induced by epithelial cadherin expression suppresses transformed growth in a ROCK-dependent manner. We also found that the induction of entosis by overexpression of epithelial cadherins is linked to the polarized distribution of Rho activity and contractile actomyosin, which is dependent on the recruitment of p190A Rho-GTPase-activating protein (p190A RhoGAP) to epithelial junctions. Together these data demonstrate that homotypic tumor cell cannibalism is induced in breast tumor cells by the establishment of epithelial cell-cell junctions through the mechanism of entosis.

Results

Expression of epithelial cadherins induces entosis in human tumor cells

Although cell cannibalism has been observed between breast tumor cells in human cancers [7, 13], we noted that the majority of human breast tumor cell lines that we examined did not exhibit engulfed cell structures and did not undergo entosis when cultured in suspension, a condition that induces entosis [13] (Figure 1A). Many human breast tumors express the epithelial cadherin proteins E-cadherin [19] or P-cadherin [20]. However, we found that many human breast tumor cell lines lacked epithelial cadherin expression (Figure 1B and Supplementary information, Figure S1A) and were deficient in entosis (Figure 1A). Expression of exogenous epithelial cadherins (E- or P-cadherin) in such cells suppressed cell scattering and induced epithelial morphology in adherent cultures, and facilitated cell clustering in suspension (Supplementary information, Figure S1A and S1B). Importantly, the introduction of E- or P-cadherin also induced entosis between tumor cells cultured in the absence of matrix adhesion (Figure 1C and 1D). Overexpression of epithelial cadherins in MDA-MB-231 and MDA-MB-453 tumor cells was especially effective in inducing the formation of cannibalistic cell structures, reaching similar frequencies observed in non-tumor MCF10A cells that are known to undergo entosis [13] (Figure 1D and Supplementary information, Movie S1). Cells that were engulfed following the expression of epithelial cadherins underwent entotic cell death, which was demonstrated by the recruitment of the autophagy protein microtubule-associated protein 1 light chain 3 (LC3) to entotic vacuoles, and by cell death inhibition upon treatment with the PI3-kinase class III inhibitor 3-methyladenine (3-MA) or upon siRNA-mediated depletion of the autophagy proteins Atg5 and Atg7, as previously reported [14] (Supplementary information, Figure S2A and S2B). Entosis and entotic cell death occurred at a high frequency when adhesion-restored MDA-MB-453 cells were cultured in soft agar (Figure 2C, 2D, and Supplementary information, Figure S2C and Movie S2). The expression of epithelial cadherins neither affected cell division rates nor induced non-entotic cell death in soft agar (Figure 2A, 2B, 2E, and Supplementary information, Figure S2D), but suppressed colony formation (Figure 2F and 2G). Taken together, these data suggest that restoration of epithelial adhesion is sufficient to induce entosis in human tumor cells, and the induction of cell cannibalism by entosis may suppress transformed growth.

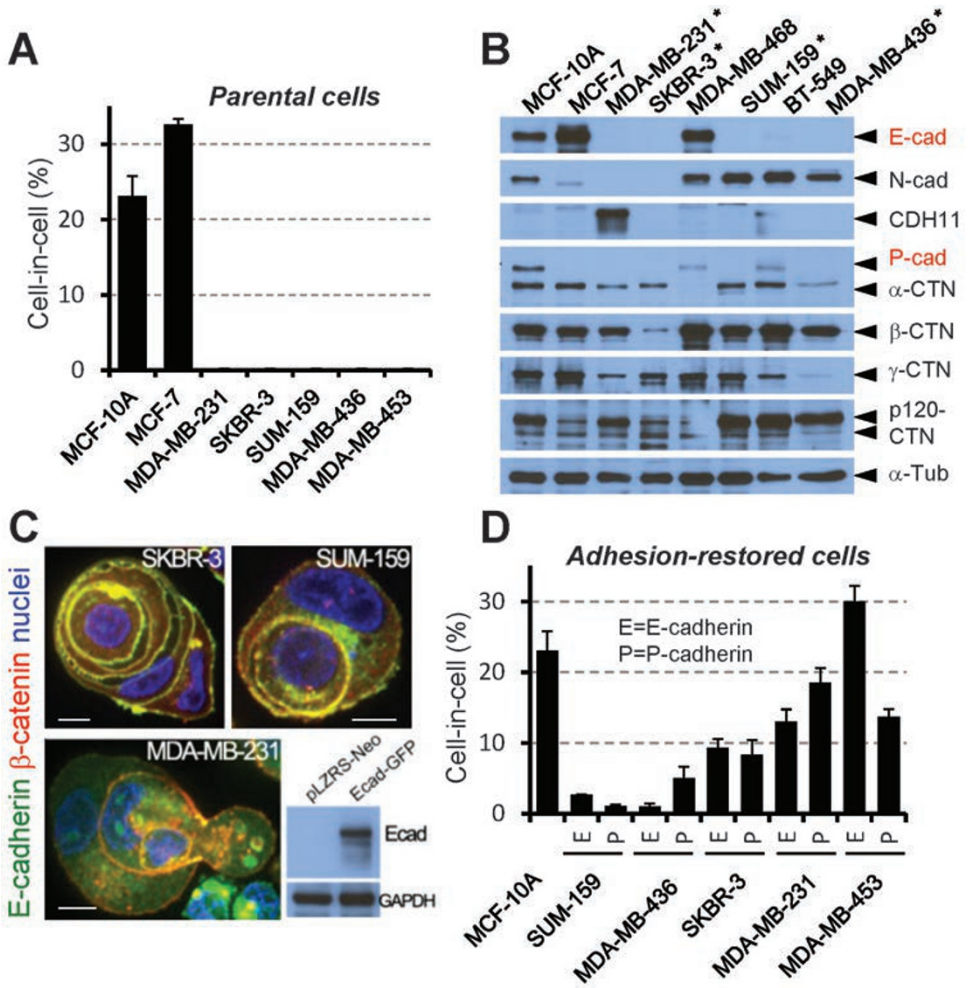

Figure 1 Restoration of epithelial cadherin expression in tumor cells induces entosis. **(A)** Frequencies of cell-in-cell formation in a panel of breast tumor cell lines as indicated. Cells were cultured in the absence of matrix adhesion for 9 h before analysis. Data are mean ± SD of triplicate experiments, *n* = 311-435 for each cell line. Note that MCF10A is a nontransformed mammary epithelial cell line. **(B)** Expression of a panel of cell-cell adhesion molecules in breast tumor cell lines. Asterisks indicate cells lacking expression of both E- and P-cadherin. Note that P-cadherin and α-catenin were blotted simultaneously. **(C)** Representative images of cell-in-cell structures formed between E-cadherin-expressing cells as indicated. Immunostaining of E-cadherin (green) and β-catenin (red), and DAPI-stained nuclei (blue) are shown. Scale bar, 10 μm. Western blot shows E-cadherin-GFP expression in MDA-MB-231 cells. Ecad, E-cadherin. Also see Supplementary information, Figure S1A and S1B for MDA-MB-453 cells. **(D)** Cell-in-cell formation in a panel of breast cancer cell lines after E- or P-cadherin expression. Cells, except for MDA-MB-453/E-cadherin (12 h), were cultured in the absence of matrix adhesion for 7-9 h before analysis. Data are mean ± SD of triplicate experiments, *n* = 300-593 for each cell line. See Supplementary information, Movie S1 for activated entosis in MDA-MB-453/P-cadherin cells.

Polarized distribution of Rho activity and contractile actomyosin during entosis

To explore the mechanism by which overexpression of epithelial cadherins induces engulfment, we examined the RhoA pathway, which is required in internalizing cells for entosis [13]. During entosis, RhoA activity measured with a FRET-based biosensor was markedly higher in the majority of internalizing cells compared to engulfing hosts, and was found at cortical regions oriented away from cell-cell junctions (Figure 3A and Supplementary information, Figure S3A). The endogenous RhoA pathway was required for entosis as siRNA-mediated knockdown of RhoA or inhibition of ROCKs (ROCK I/II) with Y27632 blocked cell-in-cell formation [13] (Supplementary information, Figure S3B and S3C). Like RhoA activity, levels of phosphorylated myosin light chain 2 at Ser19 (pMLC2), a readout of contractile myosin downstream of ROCK I/II, were also higher

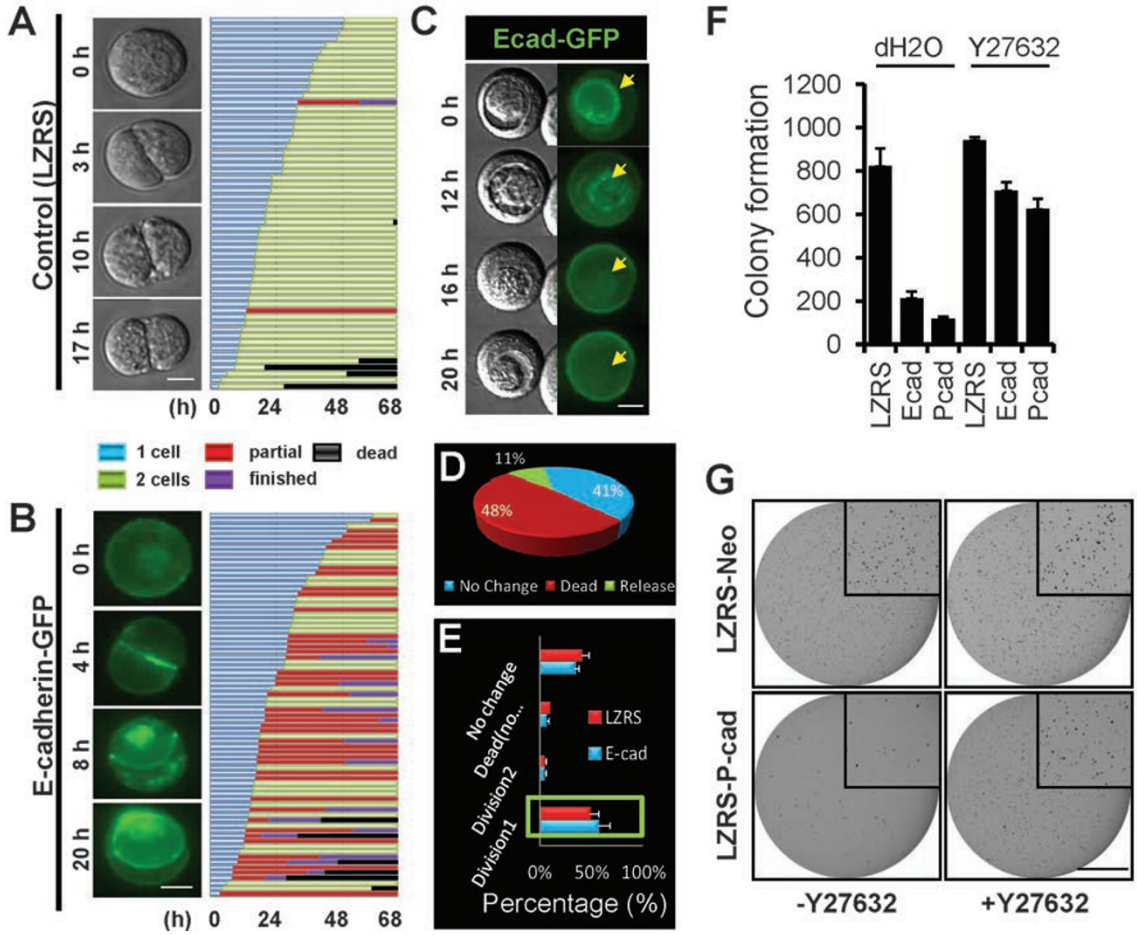

Figure 2 Suppression of transformed cell growth upon entosis induction. **(A**, **B)** Time-lapse imaging of control **(A)** and E-cadherin-expressing **(B)** MDA-MB-453 cells in soft agar. Images show cell division **(A**, **B)** followed by cell-in-cell formation marked by E-cadherin-GFP **(B)**. Bar graph shows cell fates, including division (blue and green bars), entosis (red and purple bars), and cell death (black bars) for each divided cell (Y axis) during a 68-h period (X axis). Scale bar, 10 μm. **(C)** Representative time-lapse images showing the death of internalized cells, marked by disappearance of E-cadherin-GFP (arrows). Scale bar, 10 μm. See Supplementary information, Movie S2. **(D)** Cell fates of internalized cells in E-cadherin-expressing MDA-MB-453 cells examined for 20 h in soft agar. n = 56. **(E)** Quantification of cell division and death in **A** and **B**. Division 1 refers to first cell division (one cell to two). Division 2 refers to second division (two cells to four). Dead (non-e) refers to cell death that is unrelated to entosis. No change refers to cells that remained single during the entire analysis period of 68 h. No significant differences were found between control (LZRS) and E-cadherin-expressing MDA-MB-453 cells in percentages of division 1 (P = 0.39), division 2 (P = 0.77), dead (non-e) (P = 0.06) and no change (P = 0.15). Data are mean ± SD of experiments in triplicate, and are representatives of three independent experiments. Total cell number analyzed n = 158 (E-cad) and 144 (LZRS). **(F)** Colony formation of control, E- and P-cadherin-expressing MDA-MB-453 cells in soft agar in the presence or absence of Y27632, an inhibitor that blocks entosis. Data are mean ± SD of cells analyzed in triplicate, and are representative of three independent experiments. **(G)** Representative images of colony formation of control and P-cadherin-expressing MDA-MB-453 cells in soft agar in the presence or absence of Y27632. Scale bar, 1 cm.

in the majority of internalizing cells compared to the hosts (Figure 3B). In most internalizing cells, pMLC2 was enriched in the cortex oriented away from cell-cell junctions, similar to previous reports [21, 22], or occasionally in plaques adjacent to cell-cell junctions (data not shown). This pattern was consistently observed in entotic cell structures from a variety of tumor cell types (Supplementary information, Figure S4A and S4B), as well as from cells isolated from pleural exudates of a patient with metastatic breast cancer (Supplementary information, Figure S4A). Like RhoA activity and pMLC2, actin, myosins (MHC IIA and IIB) and ROCK I/II were accumulated at higher levels in internalizing cells compared to host cells, and were enriched at the cell cortex

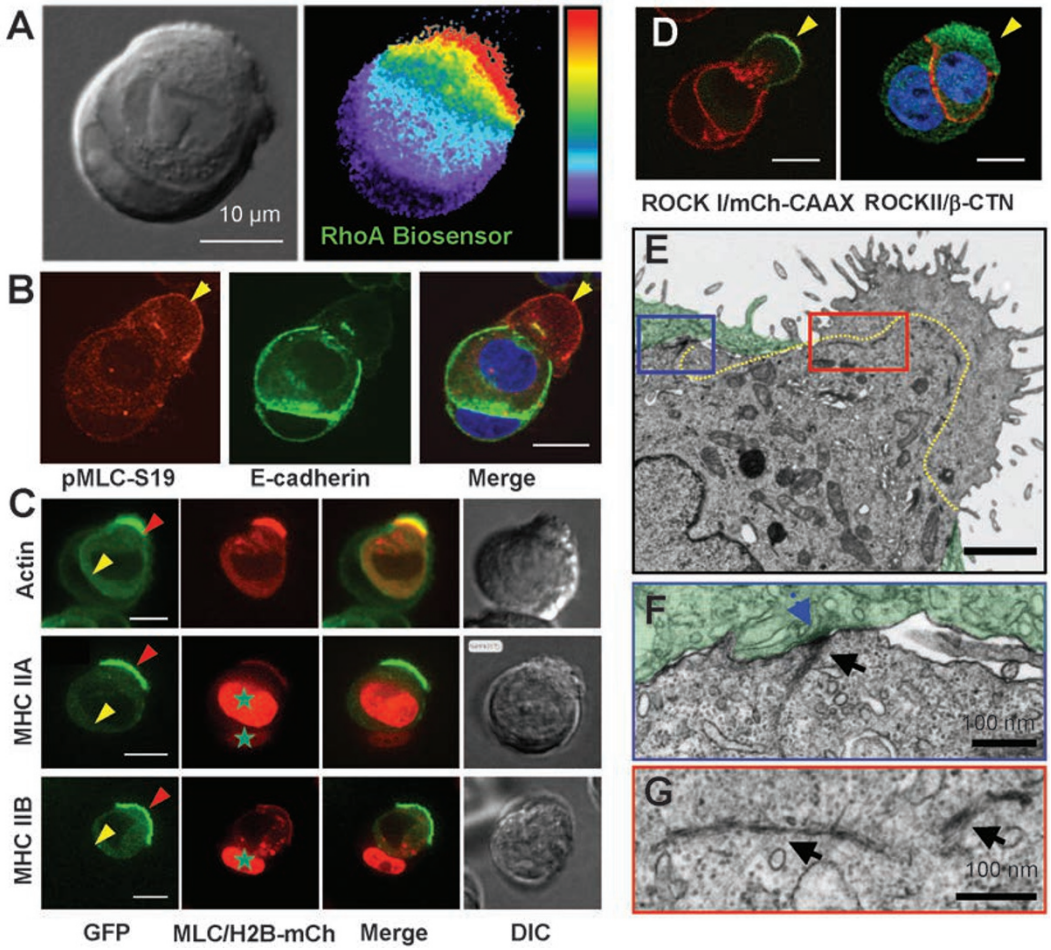

Figure 3 Polarized distribution of RhoA activity and contractile actomyosin during entosis. **(A)** Active RhoA is enriched in the cortical region of an internalizing cell away from the cell-cell junction as measured with a FRET-based biosensor in MCF10A cells. Also see Supplementary information, Figure S3A. Scale bar, 10 μm. **(B)** Distribution of pMLC2 in entotic cell structure. Panels show immunofluorescence staining of entotic structure from MCF10A for pMLC2 (red), and E-cadherin (green) to highlight the cell-cell junction. Arrowheads indicate strong staining at the cortex of the internalizing cell distal to the cell-cell adhesion labeled with E-cadherin. Scale bar, 10 μm. See Supplementary information, Figure S4A and S4B for staining in other cells. **(C)** Asymmetric distribution of GFP-tagged actin and myosin heavy chains (MHC IIA and IIB) in intermediate entotic cell structures of MCF10A cells. Red arrowheads indicate the distal cortical regions, and yellow arrowheads show cell-cell contact regions. H2B-mCherry (mCh) was expressed in some cells to indicate the nuclei (green star). Scale bar, 10 μm. **(D)** Distribution of ROCKs in entotic cell structure. Polarized localization of ROCK I-GFP (left panel) and ROCK II (immunofluorescence of ROCK II, right panel) at the distal cortical region of the internalizing MCF10A cells. Cell contacts are indicated in red by mCherry-CAAX fluorescence or β-catenin immunostaining. Scale bar, 10 μm. **(E)** A representative TEM image of the cortical region of an internalizing cell distal from cell-cell junction. Blue box indicates adherens junction region. Red box indicates localization of filamentous actin structures. Yellow dashed line indicates filamentous actin structure across the distal cortex of the internalizing MCF10A cell. Outer cell is shaded in green. Scale bar, 500 nm. See Supplementary information, Figure S5 for whole view of entotic cell structure. **(F)** Cropped view of the region boxed in blue from **E**. Blue arrowhead indicates adherens junction, and black arrow indicates filamentous actin structure. Outer cell is shaded in green. Scale bar, 100 nm. **(G)** Cropped region boxed in red from **E**. Arrows indicate filamentous actin structures. Scale bar, 100 nm.

oriented away from cell-cell adhesions (Figure 3C and 3D). By transmission electron microscopy (TEM), actin structures were observed to accumulate within the internalizing cell, emanating away from cell-cell junctions (Figure 3E-3G and Supplementary information, Figure S5).

To examine whether the accumulation of actomyosin could serve as a marker to identify engulfed sibling cells

during transformed growth, we performed time-lapse imaging of the localization of mCherry-tagged MLC in cells cultured in soft agar. Following the cell division, mCherry-MLC fluorescence was excluded from the cell-cell junction formed between siblings and localized predominantly to the cell cortex (Figure 4A, 3:30). Notably, internalizing cells accumulated more mCherry-MLC fluorescence at the cortex compared to host cells (Figure 4A, 8:30) and were then engulfed (Figure 4A, 9:30 to 11:30), suggesting that changes in cortical actomyosin of daughter cells dictate the identity of engulfed cells. Consistently, inhibition of ROCK I/II with Y27632 rapidly abolished the polarized accumulation of actin and MLC at the cortex of internalizing cells and blocked entosis (Figure 4B). Importantly, Y27632 treatment also restored the transformed growth of cadherin-expressing tumor cells in soft agar (Figure 2F and 2G). Taken together, these observations suggest that entosis is driven by differences in polarized ROCK-regulated cortical actomyosin, which in turn suppresses the transformed growth of cells expressing epithelial cadherins.

p190A RhoGAP is required for entosis and the polarized distribution of myosin

We next attempted to explore how the polarized distribution of Rho activity is established. We hypothesized that recruitment of a RhoGAP to the epithelial cell junction might restrict the local activity of Rho and contractile myosin, leaving high levels of activity at the cortex oriented away from cell adhesions. To investigate regulators of Rho signaling that could potentially control entosis, we knocked down candidate GAPs that were reported to affect cell-cell junctions [23-26], including Deleted in Liver Cancer 1 (DLC1), p190A RhoGAP (p190A), and Leukemia-associated RhoGEF (LARG, a GAP for trimeric G proteins 12/13 and q), and examined the effects on entosis. Of these candidates, only the knockdown of p190A with siRNA reduced cell-cell adhesion and induced the scattering of matrix-attached cells (Figure 5A and 5B), and only p190A knockdown

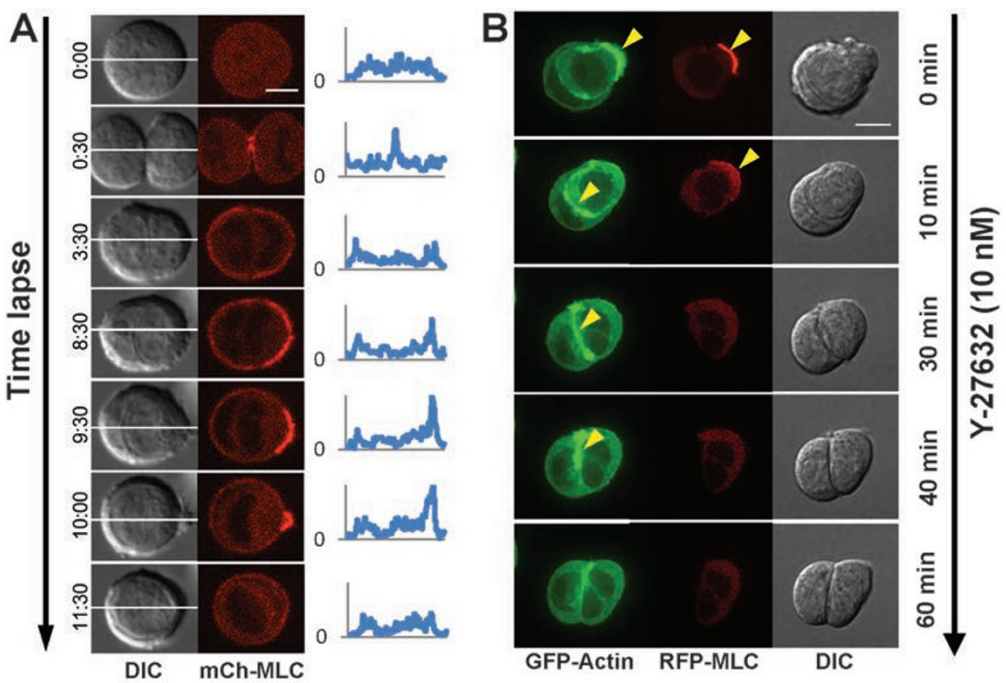

Figure 4 Polarized distribution of actomyosin is required for entosis. **(A)** Left panels show DIC and red fluorescence images of cell division in soft agar followed by entotic structure formation between sibling MCF10A cells expressing mCherry-MLC (red). Right graphs show absolute mCherry pixel intensities for the indicated line-scans (ImageJ software (NIH)). Note that mCherry-MLC intensity increases at the distal cortex of the internalizing cell from 8:30 to 10:00 compared to the outer cell. Times are indicated as hours:minutes. Scale bar, 10 μm. **(B)** ROCKI/II inhibition by Y27632 treatment abolished cortical localization of actomyosin and blocked entosis as shown by time-lapse microscopy. Images show representative of 18 intermediate cell-in-cell structures that were imaged. In all cases, the polarized pattern of actomyosin was abolished within 60 min after Y27632 treatment. Arrowheads indicate the cortical region of the internalizing cell with accumulated actin (GFP-actin) and MLC (RFP-MLC) that changes from distal to the cell-cell junction (at 0 min for actin and MLC) to proximal (by 20 min post treatment, for actin only). Scale bar, 10 μm.

inhibited entosis of cells cultured under matrix-detached conditions (Figure 5B). Knockdown of p190A with two independent shRNAs similarly reduced entosis frequencies in matrix-detached cells (Supplementary information, Figure S6A and S6B). Importantly, p190A depletion increased the growth of MCF10A-E7-Bcl2 cells in soft agar, which is known to undergo a high rate of entosis [14], consistent with an inhibitory role of entosis in transformed growth (Supplementary information, Figure S6E and S6F). Similarly, p190A depletion inhibited entosis between MDA-MB-231 breast tumor cells expressing exogenous E- or P-cadherins, and enhanced transformed growth, demonstrating that p190A RhoGAP is required for entosis and cadherin-mediated suppression of transformed growth (Supplementary information, Figure S7). As reported [25], we found that p190A was localized to cell-cell adhesions where it was colocalized with β-catenin (Figure 5C). Knockdown of p190A led to increased pMLC2 staining, a readout of Rho activity, at cell-cell adhesions (Figure 5D and Supplementary information, Figure S6C and S6D), suggesting that the recruitment of p190A to epithelial adhesions spatially restricts Rho pathway activity and inhibits myosin contraction at cell-cell junctions, which promotes entosis.

Discussion

Here we demonstrate that expression of epithelial E- or P-cadherins is sufficient to activate the cell cannibalism program entosis in breast tumor cells. Notably, expression of exogenous epithelial cadherins induced high levels of entosis in matrix-detached MDA-MB-453 and MDA-MB-231 tumor cells, with frequencies comparable to those previously observed in non-tumor MCF10A cells which require endogenous E- and P-cadherins to execute entosis [13]. Upon expression of epithelial cadherins, entosis was also induced to a moderate level in SKBR-3 cells, and to lower levels in MDA-MB-436 and SUM-159 tumor cells. These differences in entosis frequencies upon exogenous cadherin expression may

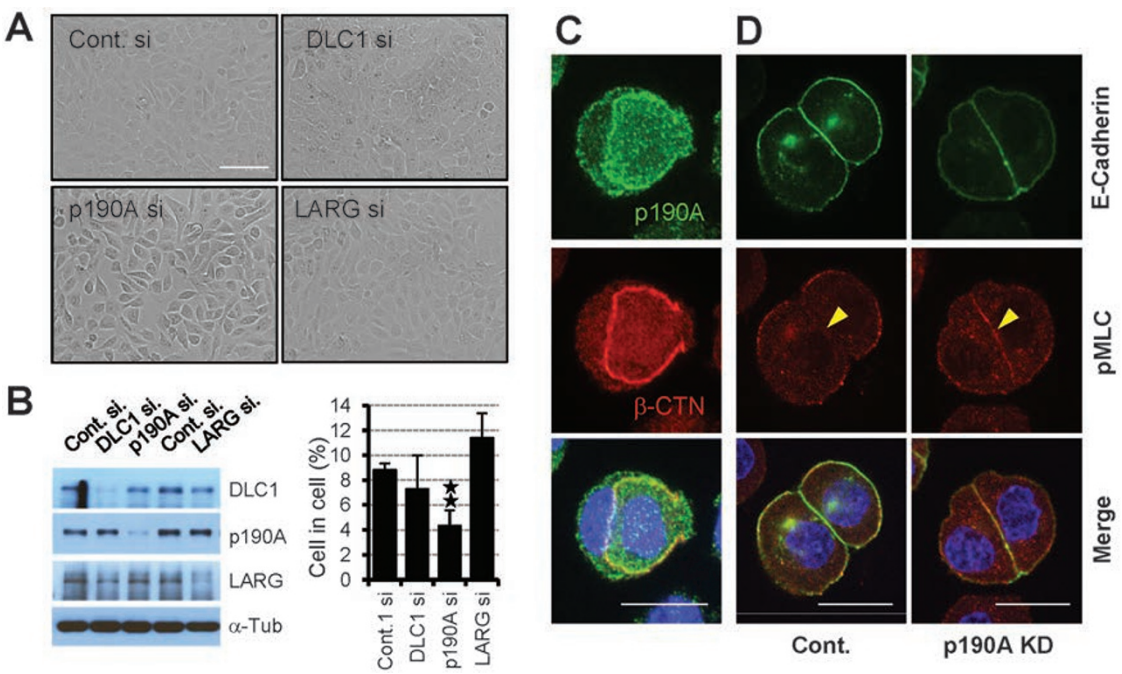

Figure 5 p190A RhoGAP is required for entosis. **(A)** Representative images of different siRNA (si)-transfected MCF10A cells as indicated. Scale bar, 50 μm. **(B)** Knockdown of p190A RhoGAP inhibits entosis. Left panel shows expression of different GAPs in MCF10A cells upon siRNA transfection by western blotting. Right panel shows quantification of entotic cell structures upon knockdown of different GAPs as indicated. Cells were cultured in suspension for 6 h. Data are mean ± SD of triplicate experiments, $n > 300$ for each group. Two stars, $P < 0.01$ as compared with control. Also see Supplementary information, Figure S6A and S6B. **(C)** Junctional localization of p190A RhoGAP. Panels show immunofluorescence staining for p190A RhoGAP (green), and β-catenin (β-CTN, red) to highlight cell-cell junction in MCF10A cells undergoing entosis. Scale bar, 20 m. **(D)** Junctional localization of pMLC2 upon p190A RhoGAP depletion (p190A KD), as detected by immunofluorescence staining of MCF10A cell doublets for pMLC2 (red), and E-cadherin (green) to show cell junctions. Scale bar, 20 μm. Arrowheads indicate pMLC2 staining at cell junctions. Please also see Supplementary information, Figure S6C and S6D.

reflect different permissivity of different genetic backgrounds to restored adhesion, or differences in Rho-GTPase activity in tumor cells. In cells with restored entosis, engulfed cells underwent entotic cell death associated with the recruitment of the autophagy protein LC3 to entotic vacuoles [14], and such cell death was in part dependent on autophagy proteins, similar to what we have reported for non-tumor MCF10A cells [13, 14], demonstrating that breast tumor cells retain the capacity to mediate this form of cell death when epithelial adhesion is restored. Interestingly, engulfed cells committed to multiple fates other than cell death, such as escaping from their hosts. Taken together, these data suggest that the ectopic expression of epithelial cadherins is sufficient to restore entosis and entotic cell death in breast tumor cells.

Our data demonstrate that a high level of entosis induced by expression of epithelial cadherins is associated with the inhibition of transformed growth of tumor cells in a ROCK-dependent manner, suggesting that entosis serves as a mechanism of tumor suppression. E-cadherin is a known tumor suppressor whose inactivation has been shown to promote cell proliferation, anoikis resistance, invasion, primary tumor growth, and metastasis [27-30]. Accordingly, the E-cadherin gene *CDH1* is lost or mutated in some human breast cancers, particularly those of the lobular subtype [31, 32]. Entosis is another mechanism by which the expression of E-cadherin limits transformed growth by inducing cell death. However, many breast tumors including the most invasive ductal carcinomas and metastatic tumors retain E-cadherin expression, and E-cadherin may promote tumor progression by supporting cell survival, collective modes of invasion, or the outgrowth of metastatic tumors that may be promoted by an epithelial rather than mesenchymal phenotype [19, 33-39]. Like E-cadherin, P-cadherin is also expressed in some breast cancers and is a poor prognostic indicator [20]. We have shown that in addition to causing cell death that limits transformed growth, entosis can also (1) induce aneuploidy by disrupting cytokinesis [7], (2) support cell survival under nutrient-limiting conditions [10], and (3) promote cell competition that could contribute to clonal progression (see the companion paper by Sun *et al*. [12]), suggesting that this cannibalistic cell behavior could conceivably promote tumor progression in the long term, and could potentially contribute to some of the tumor-promoting activities of epithelial cadherins.

We provide evidence that epithelial cadherins induce entosis in part by spatially restricting contractile actomyosin to the cortex that is distal from cell-cell adhesions, which is dependent on p190A RhoGAP that is recruited to cell-cell junctions (Figure 6). This spatial positioning of contractile myosin and RhoA activity is reminiscent of patterns identified during formation of adhesions between pairs of matrix-attached cells [40]. Thus, entosis may result from imbalance of actomyosin contraction that is normally associated with cell-cell adhesion, as previously proposed [13]. Previously it was reported that p120 catenin, a cytoplasmic binding partner of cadherin proteins, can directly interact with p190A, which mediates recruitment of this RhoGAP to cell junctions [25]. We thus propose that p190A RhoGAP is recruited to junctions between cells that are involved in entosis (host and internalizing cells), as an asymmetric distribution of actomyosin could be identified in both cells (Figures 3-5). The local inhibition of myosin contraction at cell-cell junctions may act in concert with the promotion of Rho activity and actomyosin accumulation by PDZ-RhoGEF at the invading cell tail, as recently reported [22], to establish the polarized contraction necessary for entosis. In addition, we have found that tumor cells expressing mesenchymal-type cadherins, N-cadherin and cadherin-11, did not exhibit cell-in-cell structures but are nevertheless competent for entosis once E- or P-cadherin are introduced. This difference may relate to factors other than p190A RhoGAP as this RhoGAP can also be recruited to N-cadherin-mediated cell junctions [25]. Therefore, it will be interesting to study why mesenchymal-type cadherins are unable to mediate entosis in breast tumor cells.

Our data demonstrate that cell cannibalism can be induced in a panel of breast tumor cell lines upon expression of epithelial cadherins, which supports the idea that entosis is an important mechanism of cell engulfment between tumor cells. In addition to homotypic cannibalism between tumor cells, E-cadherin has also been shown to mediate the engulfment of natural killer (NK) cells by tumor cells, demonstrating that homophyllic cell adhesion molecules can mediate heterotypic cannibalism as well [16]. While cadherin-based engulfment involving an active role of internalizing cells clearly represents one mechanism for tumor cell cannibalism, other mechanisms might exist as proposed for pancreatic tumor cells that engulf each other by a phagocytosis-like mechanism [17], and for metastatic melanoma cells that have been shown to ingest live lymphocytes by a nonphagocytosis mechanism involving ezrin and caveolae [8]. Interestingly, ezrin is also required by tumor cells for E-cadherin-dependent ingestion of live NK cells, suggesting that these apparently different forms of cell cannibalism may indeed share some mechanistic similarities [16]. Future studies aimed at localizing the Rho-family GTPase activities and cytoskeletal changes that drive engulfment

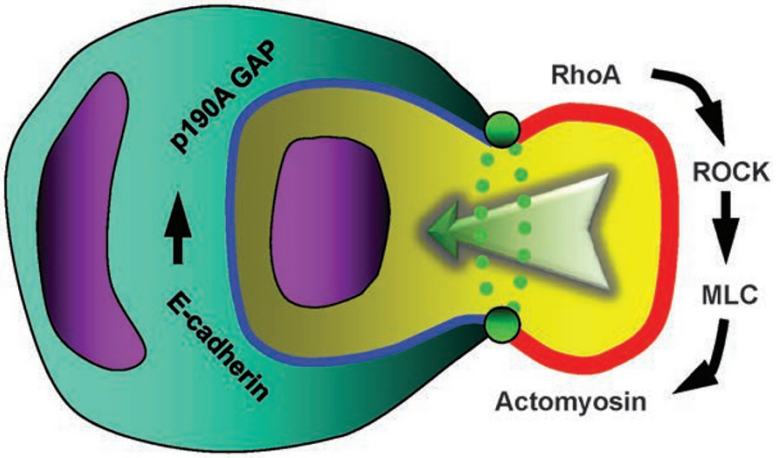

Figure 6 Model of entosis by polarized RhoA activity and actomyosin. Formation of adherens junctions mediated by epithelial cadherins (E-, or P-cadherin) results in inhibited Rho activity at cell junctions due to p190A RhoGAP recruitment to this region, which leads to polarized distribution of Rho activity that is higher at the cortical region distal to cell adhesions, generating an inward force through actomyosin contraction at the cortical region. As a result, cells with higher Rho activity will "invade" into neighbors to form cell-in-cell structures.

may shed light on whether different forms of cell cannibalism that have been observed in human tumors occur through shared or distinct mechanisms.

Materials and Methods

Cells and culture conditions

MCF7, MCAS, PancTu, VmCUB3, 575A, Caco2, 293FT, SUM159 cells, and their derivatives were maintained in Dulbecco's modified Eagle's medium (DMEM) supplemented with 10% FBS (Sigma). SKBR3 and its derivative lines were maintained in McCoy's 5A medium supplemented with 10% FBS. MDA-MB-231, MDA-MB-453, MDA-MB-436, and their derivative lines were maintained in Leibovitz's L-15 (Invitrogen) supplemented with 10% FBS. MCF10A and its derivative cells were cultured in DMEM/F12 with 5% horse serum (Atlanta Biologicals), 20 ng/ml EGF (Peprotech), 10 μg/ml insulin (Sigma), 0.5 μg/ml hydrocortisone (Sigma), and 100 ng/ml cholera toxin (Sigma).

Antibodies and chemical reagents

Antibodies with working dilution factors, company source, and catalog number are listed as below: anti-tubulin (1:5 000; Sigma; T5168), anti-pMLC (1:200 or 1 000; Cell Signaling; #3671), anti-E-cadherin (1:200 or 1:1 000; BD Biosciences; BD610181), anti-P-cadherin (1:1 000; Cell Signaling; #2189), anti-N-cadherin (1:1 000; BD Biosciences; BD610920), anti-CDH11 (1:500; Invitrogen; 32-1700), anti-α-catenin (1:1 000; BD Biosciences; BD610193), anti-β-catenin (1:200 or 1:1 000; Sigma; C2206), anti-γ-catenin (1:1 000; Cell Signaling; #2309), anti-p120-catenin (1:500; BD Biosciences; BD610133), anti-ROCK II (1:200; Upstate; 07-443), anti-DLC1 (1:200; Santa Cruz; sc-32931), anti-LARG (1:200; Abcam; ab101718), anti-p190A (1:500; BD Biosciences; BD610150), anti-ATG5 (1:1 000; Cell Signaling; #8540), and anti-ATG7 (1:1 000; Cell Signaling; #2631). Secondary antibodies include Alexa Fluor 568 anti-rabbit (1:300; Invitrogen; A11036) and Alexa Fluor 488 anti-mouse (1:300; Invitrogen; A11029). ROCK inhibitor Y27632 was purchased from TOCRIS (1254) and used at a final concentration of 10 μM. DAPI and 3-MA were purchased from Sigma (D8417 and M9281).

Immunostaining and immunoblotting

Immunostaining and immunoblotting were performed as previously described [41, 42].

Constructs

pGFP-ROCK I [43] was a gift from Dr Erik Sahai (LRI, UK). pLZRS-P-cadherin was a gift from Dr Keith R Johnson (UNMC, USA). pBabe-GFP-LC3 was a gift from Dr Xuejun Jiang (MSKCC, USA). pBabe-RhoA biosensor [44] was a gift from Dr Klaus Hahn from Addgene (12602). pEGFP-MHC IIA and IIB were gifts from Dr Tatiana Omelchenko in the lab of Dr Alan Hall. RFP-MLC [45] was a gift from Dr Michael Sheetz (Columbia University, USA). pBabe-mCherry-MLC was cloned by PCR amplification of MLC from RFP-MLC and insertion of mCherry-MLC into the *Bam*HI-*Xho*I sites of pBabe-Puro. The RNA interference hairpin constructs for human p190A GAP (sh550 and sh553) were purchased from the research facility of Memorial Sloan-Kettering Cancer Center.

Virus production and infection

Virus production and infection were performed as previously described [13]. Virus-infected cells were selected with puromycin or G418 of appropriate concentrations according to the constructs used. Fluorescent protein-expressing cells were sorted by flow cytometry if needed.

Transfection and nucleofection

siGenome SMART pool siRNAs against control (the nontargeting control siRNA, NCsi) and human RhoA, Atg5,

Atg7, DLC1, LARG, and p190A RhoGAP were obtained from Dharmacon. siRNA transfection was performed as previously described [13]. Cell analyses were performed 48 h post transfection. For nucleofection, 1×10^6 MCF10A cells were transduced with 6 μg target plasmid by program T-24 using Nucleofector Solution V reagent (Lonza), and cell analyses were performed 12 h post nucleofection except unless otherwise specifically indicated.

Time-lapse microscopy in soft agar

To follow cell division and entosis in soft agar, cells (1×10^5 for each) were mixed together and embedded into growth media + 0.4% low melt agarose (Sigma), and plated onto glass-bottomed dishes (MatTek) precoated with polyhema (Sigma, P3932) to prevent cell adherence. Isolated cells or cell pairs were chosen for imaging at the start of the analyses. Images were acquired for DIC and fluorescence channels every 10-15 min using a Nikon Ti-E inverted microscope attached to a CoolSNAP CCD (charge-coupled device) camera (Photometrics). The timing of cell death was judged morphologically by the appearance of a broken cell membrane, or cessation of cell movement, or both. The formation of cell-in-cell structures was determined morphologically by the appearance of cell-cell junctions by DIC and E-cadherin-GFP as described [42]. Cell structures with greater than half of one cell body internalized into a neighboring cell were counted as "partial", and cell structures with junctions that enwrapped neighboring cells completely were scored as "finished".

Anchorage-independent growth

To examine transformed growth [46], cells (5 000 cells) were embedded into growth media + 0.4% low melting agarose (Sigma), and plated onto preformed growth media + 0.5% agarose pads in 6-well plates. 1 ml of full media with or without Y27632 was added after agarose was solidified at room temperature. Medium was changed once a week for 2 weeks. Colonies were stained with 0.02% iodonitrotetrazolium chloride (Sigma) and quantified using an Optronix Gelcount colony counter (Oxford Optronix).

FRET

Briefly, RhoA activity was measured by monitoring the ratio of ECFP to Citrine-YFP FRET and ECFP intensities as previously described [44]. Also see Supplementary information, Data S1 for a more detailed protocol.

Statistics

P values were calculated by two-tailed Student's *t*-test using Excel or GraphPad Prism 5 software.

Acknowledgments

We thank Drs Alan Hall and Xuejun Jiang and their lab members, and members of the Overholtzer laboratory for reagents and discussions on the manuscript. We thank Drs Keith R Johnson, Klaus Hahn, Michael Sheetz, Erik Sahai, and Tingchao Chou for reagents. This work was supported by grants from the NCI (CA154649, MO), the NIGMS (GM09312, LH), the Geoffrey Beene Cancer Research Center at MSKCC (MO), the Louis V Gerstner, Jr Young Investigators Fund (MO), the Benjamin Friedman Research Fund (MO), the National Basic Research Program of China (2015CB553704, QS), and the National Natural Science Foundation of China (30871364 and 81472588, QS).

References

1 Hochreiter-Hufford A, Ravichandran KS. Clearing the dead: apoptotic cell sensing, recognition, engulfment, and digestion. *Cold Spring Harb Perspect Biol* 2013; **5**:a008748.
2 Hoeppner DJ, Hengartner MO, Schnabel R. Engulfment genes cooperate with ced-3 to promote cell death in *Caenorhabditis elegans*. *Nature* 2001; **412**:202-206.
3 Reddien PW, Cameron S, Horvitz HR. Phagocytosis promotes programmed cell death in *C. elegans*. *Nature* 2001; **412**:198-202.
4 Neniskyte U, Brown GC. Lactadherin/MFG-E8 is essential for microglia-mediated neuronal loss and phagoptosis induced by amyloid beta. *J Neurochem* 2013; **126**:312-317.
5 Brown GC, Neher JJ. Eaten alive! Cell death by primary phagocytosis: 'phagoptosis'. *Trends Biochem Sci* 2012; **37**:325-332.
6 Overholtzer M, Brugge JS. The cell biology of cell-in-cell structures. *Nat Rev Mol Cell Biol* 2008; **9**:796-809.
7 Krajcovic M, Johnson NB, Sun Q, *et al.* A non-genetic route to aneuploidy in human cancers. *Nat Cell Biol* 2011; **13**:324-330.
8 Lugini L, Matarrese P, Tinari A, *et al.* Cannibalism of live lymphocytes by human metastatic but not primary melanoma cells. *Cancer Res* 2006; **66**:3629-3638.
9 Abodief WT, Dey P, Al-Hattab O. Cell cannibalism in ductal carcinoma of breast. *Cytopathology* 2006; **17**:304-305.
10 Krajcovic M, Krishna S, Akkari L, Joyce JA, Overholtzer M. mTOR regulates phagosome and entotic vacuole fission. *Mol Biol Cell* 2013; **24**:3736-3745.
11 Chen YH, Wang S, He MF, *et al.* Prevalence of heterotypic tumor/immune cell-in-cell structure *in vitro* and *in vivo* leading to formation of aneuploidy. *PLoS One* 2013; **8**:e59418.
12 Sun Q, Luo T, Ren Y, *et al.* Competition between human cells by entosis. *Cell Res* 2014; **24**:1299-1310.
13 Overholtzer M, Mailleux AA, Mouneimne G, *et al*. A nonapoptotic cell death process, entosis, that occurs by cell-in-cell invasion. *Cell* 2007; **131**:966-979.
14 Florey O, Kim SE, Sandoval CP, Haynes CM, Overholtzer M. Autophagy machinery mediates macroendocytic processing and entotic cell death by targeting single membranes. *Nat Cell Biol* 2011; **13**:1335-1343.
15 Sharma N, Dey P. Cell cannibalism and cancer. *Diagn Cytopathol* 2011; **39**:229-233.
16 Wang S, Guo Z, Xia P, *et al.* Internalization of NK cells into tumor cells requires ezrin and leads to programmed cell-in-cell death. *Cell Res* 2009; **19**:1350-1362.
17 Cano CE, Sandi MJ, Hamidi T, *et al.* Homotypic cell cannibalism, a cell-death process regulated by the nuclear protein 1, opposes to metastasis in pancreatic cancer. *EMBO Mol Med* 2012; **4**:964-979.
18 Abreu M, Sealy L. Cells expressing the C/EBPbeta isoform, LIP, engulf their neighbors. *PLoS One* 2012; **7**:e41807.
19 Moll R, Mitze M, Frixen UH, Birchmeier W. Differential loss of E-cadherin expression in infiltrating ductal and lobular breast carcinomas. *Am J Pathol* 1993; **143**:1731-1742.

20 Liu N, Yu Q, Liu TJ, *et al.* P-cadherin expression and basal-like subtype in breast cancers. *Med Oncol* 2012; **29**:2606-2612.
21 Wan Q, Liu J, Zheng Z, *et al.* Regulation of myosin activation during cell-cell contact formation by Par3-Lgl antagonism: entosis without matrix detachment. *Mol Biol Cell* 2012; **23**:2076-2091.
22 Purvanov V, Holst M, Khan J, Baarlink C, Grosse R. G-protein-coupled receptor signaling and polarized actin dynamics drive cell-in-cell invasion. *Elife* 2014 June 20. doi: 10.7554/eLife.02786
23 Noren NK, Arthur WT, Burridge K. Cadherin engagement inhibits RhoA via p190RhoGAP. *J Biol Chem* 2003; **278**:13615-13618.
24 Bourguignon LY, Gilad E, Brightman A, Diedrich F, Singleton P. Hyaluronan-CD44 interaction with leukemia-associated RhoGEF and epidermal growth factor receptor promotes Rho/Ras co-activation, phospholipase C epsilon-Ca2+ signaling, and cytoskeleton modification in head and neck squamous cell carcinoma cells. *J Biol Chem* 2006; **281**:14026-14040.
25 Wildenberg GA, Dohn MR, Carnahan RH, *et al.* p120-catenin and p190RhoGAP regulate cell-cell adhesion by coordinating antagonism between Rac and Rho. *Cell* 2006; **127**:1027-1039.
26 Simoes S, Denholm B, Azevedo D, *et al.* Compartmentalisation of Rho regulators directs cell invagination during tissue morphogenesis. *Development* 2006; **133**:4257-4267.
27 Derksen PW, Liu X, Saridin F, *et al.* Somatic inactivation of E-cadherin and p53 in mice leads to metastatic lobular mammary carcinoma through induction of anoikis resistance and angiogenesis. *Cancer Cell* 2006; **10**:437-449.
28 Onder TT, Gupta PB, Mani SA, *et al.* Loss of E-cadherin promotes metastasis via multiple downstream transcriptional pathways. *Cancer Res* 2008; **68**:3645-3654.
29 Perrais M, Chen X, Perez-Moreno M, Gumbiner BM. E-cadherin homophilic ligation inhibits cell growth and epidermal growth factor receptor signaling independently of other cell interactions. *Mol Biol Cell* 2007; **18**:2013-2025.
30 Frixen UH, Behrens J, Sachs M, *et al.* E-cadherin-mediated cell-cell adhesion prevents invasiveness of human carcinoma cells. *J Cell Biol* 1991; **113**:173-185.
31 Heselmeyer-Haddad K, Berroa Garcia LY, Bradley A, *et al.* Single-cell genetic analysis of ductal carcinoma *in situ* and invasive breast cancer reveals enormous tumor heterogeneity yet conserved genomic imbalances and gain of MYC during progression. *Am J Pathol* 2012; **181**:1807-1822.
32 Cancer Genome Atlas N. Comprehensive molecular portraits of human breast tumours. *Nature* 2012; **490**:61-70.
33 Ionescu Popescu C, Giusca SE, Liliac L, *et al.* E-cadherin expression in molecular types of breast carcinoma. *Rom J Morphol Embryol* 2013; **54**:267-273.
34 Kowalski PJ, Rubin MA, Kleer CG. E-cadherin expression in primary carcinomas of the breast and its distant metastases. *Breast Cancer Res* 2003; **5**:R217-R222.
35 Rodriguez FJ, Lewis-Tuffin LJ, Anastasiadis PZ. E-cadherin's dark side: possible role in tumor progression. *Biochim Biophys Acta* 2012; **1826**:23-31.
36 Tsai JH, Donaher JL, Murphy DA, Chau S, Yang J. Spatiotemporal regulation of epithelial-mesenchymal transition is essential for squamous cell carcinoma metastasis. *Cancer Cell* 2012; **22**:725-736.
37 Ocana OH, Corcoles R, Fabra A, *et al.* Metastatic colonization requires the repression of the epithelial-mesenchymal transition inducer Prrx1. *Cancer Cell* 2012; **22**:709-724.
38 Chu K, Boley KM, Moraes R, Barsky SH, Robertson FM. The paradox of E-cadherin: role in response to hypoxia in the tumor microenvironment and regulation of energy metabolism. *Oncotarget* 2013; **4**:446-462.
39 Xiang X, Deng Z, Zhuang X, *et al.* Grhl2 determines the epithelial phenotype of breast cancers and promotes tumor progression. *PLoS One* 2012; **7**:e50781.
40 Yamada S, Nelson WJ. Localized zones of Rho and Rac activities drive initiation and expansion of epithelial cell-cell adhesion. *J Cell Biol* 2007; **178**:517-527.
41 Sun Q, Zhang Y, Yang G, *et al.* Transforming growth factor-beta-regulated miR-24 promotes skeletal muscle differentiation. *Nucleic Acids Res* 2008; **36**:2690-2699.
42 Sun Q, Overholtzer M. Methods for the study of entosis. *Methods Mol Biol* 2013; **1004**:59-66.
43 Pinner S, Sahai E. PDK1 regulates cancer cell motility by antagonising inhibition of ROCK1 by RhoE. *Nat Cell Biol* 2008; **10**:127-137.
44 Pertz O, Hodgson L, Klemke RL, Hahn KM. Spatiotemporal dynamics of RhoA activity in migrating cells. *Nature* 2006; **440**:1069-1072.
45 Tamada M, Perez TD, Nelson WJ, Sheetz MP. Two distinct modes of myosin assembly and dynamics during epithelial wound closure. *J Cell Biol* 2007; **176**:27-33.
46 Zhang Y, Fan KJ, Sun Q, *et al.* Functional screening for miRNAs targeting Smad4 identified miR-199a as a negative regulator of TGF-beta signalling pathway. *Nucleic Acids Res* 2012; **40**:9286-9297.

(**Supplementary information** is linked to the online version of the paper on the *Cell Research* website.)